Influence of β-Alanine on Hairpin Polyamide Orientation in the DNA Minor Groove

by **Victor C. Rucker**, **Christian Melander**, and **Peter B. Dervan***

Division of Chemistry and Chemical Engineering, California Institute of Technology, Pasadena, CA 91125, USA

Dedicated to Professor *Jack D. Dunitz* on the occasion of his 80th birthday

Antiparallel polyamides containing 1*H*-pyrrole, 1*H*-imidazole, and 3-hydroxy-1*H*-pyrrole amino acids display a preference for minor-groove binding oriented N–C with respect to the 5′-3′ direction of the DNA helix. We find that replacement of a central Py/Py pair with a β/β pair within a ten-ring hairpin relaxes the orientation preference and, for some DNA sequences, causes the polyamide to prefer the opposite C–N orientation. Substitution of the achiral γ-aminobutanoic acid (γ) with either (*R*)(or *S*)-2-(acetylamino)-4-aminobutanoic acid moderates the orientation preference of the 2-β-2-hairpin.

1. Introduction. – Many diseases are related to aberrant gene expression, and the ability to reprogram a cell with small molecules could be important in biology and human medicine [1]. Polyamides that bind predetermined DNA sequences offer a chemical approach to control gene expression [2]. Sequence specificity depends on side-by-side pairings of aromatic rings comprising 1*H*-pyrrole (Py), 1*H*-imidazole (Im), and 3-hydroxy-1*H*-pyrrole (Hp) amino acids, which bind cooperatively in the minor groove of DNA [3][4]. An Im/Py pair targets G·C, Py/Im targets C·G, Py/Py targets A·T and T·A, and Hp/Py distinguishes T·A from A·T. Although polyamides bind antiparallel to each other, the pairing rules do not distinguish whether there should be any energetic preference for alignment of each polyamide (N–C) with respect to the DNA backbone (5′-3′) of the DNA helix. In a formal sense, the dimer $(ImPyPy)_2$ could bind 5′-WGWCW-3′ or 5′-WCWGW-3′ and still not violate the binding code. The majority of our data to date suggests that there is a modest binding preference for 5′-WGWCW-3′ over 5′-WCWGW-3′ and, hence, the polyamide dimers are aligned N–C with respect to the 5′-3′ direction of the DNA strand. This orientation preference superimposed on the pairing rules confers added specificity by breaking a potential degeneracy for recognition [5][6].

In general, six-ring, eight-ring, and ten-ring hairpin polyamides bind N–C with respect to the 5′-3′ direction of the helix [5–7]. Recent studies have shown that this alignment preference is not always enforced, with evidence that the C–N arrangement is sometimes energetically favorable [8–10]. A key issue is to understand when that energetic preference is reversed. To relax the overcurvature of hairpins containing five contiguous rings, an aliphatic β-alanine pair (β/β) is often used to replace a central Py/Py pair [11]. The aliphatic amino acid β-alanine pair (β/β) shares recognition properties similar to Py and codes for A·T base pairs for steric reasons. β-Alanine has the ability

to act as a molecular spring and to restore polyamide curvature to match the DNA minor groove. This allows for optimal H-bond donor/acceptor interactions, resulting in an increase in overall affinity and specificity. We report here that replacement of a central Py/Py ring pair by β/β in a ten-ring hairpin reverses, in several cases, the usual N−C/5′-3′ orientation preference in the minor groove of DNA. Substitution of the prochiral α-C-atom of γ-aminobutanoic acid turn unit in the hairpin can be used to favor N−C or C−N alignment with respect to the 5′-3′ direction of the DNA helix [8].

Experimental Design. – In this study, we refer to N−C/5′-3′ as *forward* orientation and C−N/5′-3′ as *reverse* orientation. As a test case for polyamide design, consider targeting the sequences 5′-GWWGG-3′ and 5′-GGWWG (where W = A or T). Implementation of the pairing rules, without regard for the orientation preference of the hairpin, gives the following sequence of antiparallel pairs that code for GWWGG: Im/Py, Py/Py, Py/Py, Im/Py, Im/Py (*Fig. 1*). An antiparallel polyamide heterodimer ImPyPyImIm/PyPyPyPyPy would then be connected by a turn residue *at either end* to afford two distinct hairpins, **1** and **2**, which bind formally the same sequence but have opposite orientations. Substitution of a central Py/Py with β/β affords similarly two different hairpins **3** and **4**, which code for the same DNA sequence, but again with opposite orientations. Our experience would suggest that complex **1**·GWWGG (N−C parallel to 5′-3′ direction of the helix) is more favorable than **2**·GWWGG. We assumed that, for the more-flexible 2-β-2 motifs **3** and **4**, this would be the case as well, *i.e.*, **3**·GWWGG is more stable than **4**·GWWGG. Rotating the same antiparallel dimer 180° through the plane of the page results in ImImPyPyIm/PyPyPyPyPy. Connecting by a γ-turn unit at either end, one now generates the same hairpins **1** and **2**, which code for a different sequence GGWWG in the reverse and forward orientations, respectively (*Fig. 1*). Substitution of a central Py/Py pair with β/β affords hairpins **3** and **4**, which

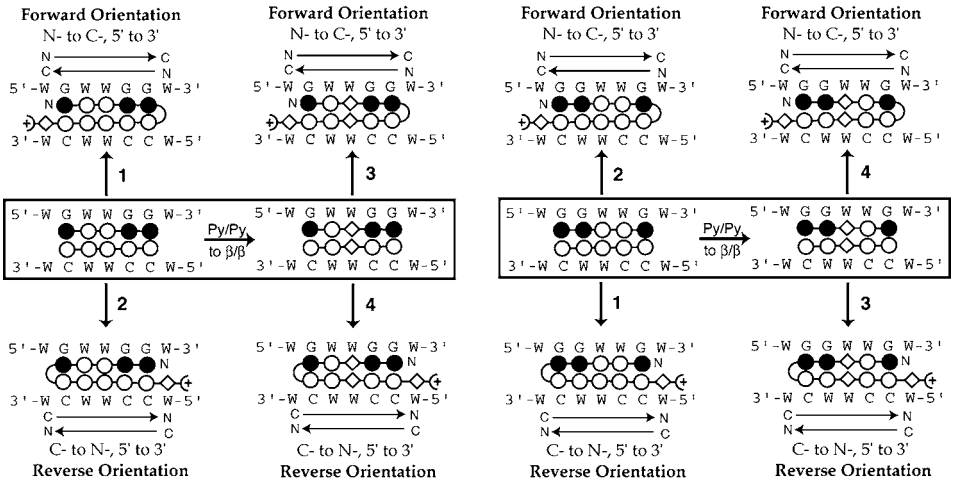

Fig. 1. *Ball-and-stick model for polyamide design.* Open circles represent 1*H*-pyrrole, black circles represent 1*H*-imidazole, and open triangles represent β-alanine.

code for GGWWG by reverse and forward orientations, respectively. Hence, there is ambiguity of sequence targeting. We examined two ten-ring hairpins **1** and **2**, and two 2-β-2 hairpins **3** and **4**, which code for GWWGG and GGWWG depending on orientation preference (*Fig. 2*). In this study, we combine quantitative footprint titration with

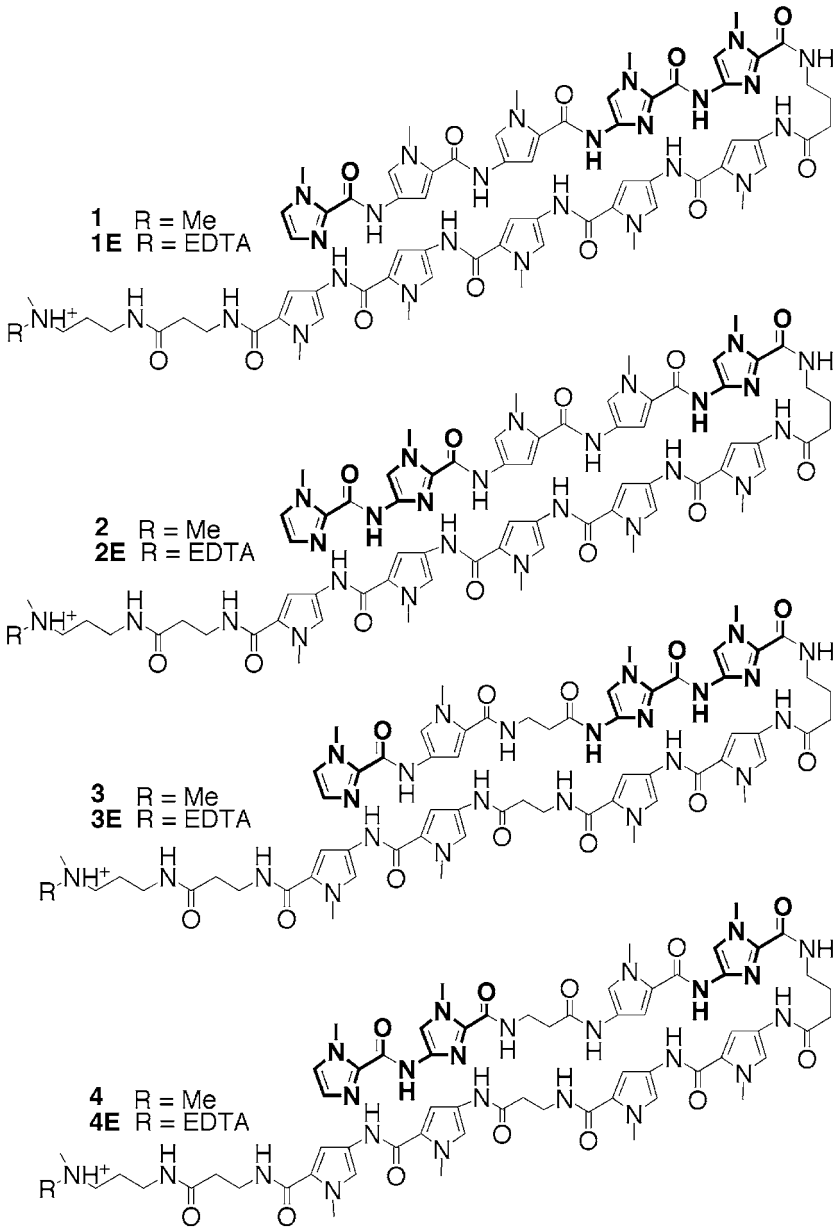

Fig. 2. *Structures of polyamides* **1**–**4**

affinity cleavage analysis to determine the energetics and orientation preferences of the two pairs of related hairpins. The equilibrium association constants were measured on a DNA fragment that contains the binding sites 5′-tAGATGGTa-3′ and 5′-tAGGTAGTa-3′. By the pairing rules, 5′-tAGATGGTa-3′ presents itself as a forward-orientation binding site for polyamides **1** and **3**, while it represents a reverse-orientation binding site for hairpins **2** and **4**. Site 5′-tAGGTAGTa-3′ represents the opposite binding preference, such that it is a forward site for **2** and **4**, and a reverse site for **1** and **3** (*Fig. 1*).

The ten-ring polyamide **1** binds both target sites 5′-tAGATGGTa-3′ and 5′-tAGGTAGTa-3′ poorly. The ten-ring polyamide **2** binds 5′-tAGGTAGTa-3′ more favorably than 5′-tAGATGGTa-3′ (*Fig. 3* and *Table 1*). This is in accord with our prior experience. Ten-ring hairpins are likely overcurved with respect to the DNA helix and require, in most cases, replacement of a central Py/Py pair with a *β*/*β* pair. The hairpins with the *β*/*β* pair, polyamides **3** and **4**, bind both target sequences. Polyamide **3** has a modest preference for 5′-tAGGTAGTa-3′ over 5′-tAGATGGTa-3′, while polyamide **4** binds both sequences within a factor of 2. Affinity-cleaving results allow us to assign the orientation preference on these two sequences (*Fig. 4*). Remarkably, ten-ring polyamide **2** prefers to bind 5′-tAGATGGTa-3′ (mismatch underlined) as a forward 2-bp mismatch, rather than a reverse orientation match. 2-*β*-2 Hairpin **3** binds both sites as pairing rules matches regardless of orientation. However, the 2-*β*-2 polyamide **4**

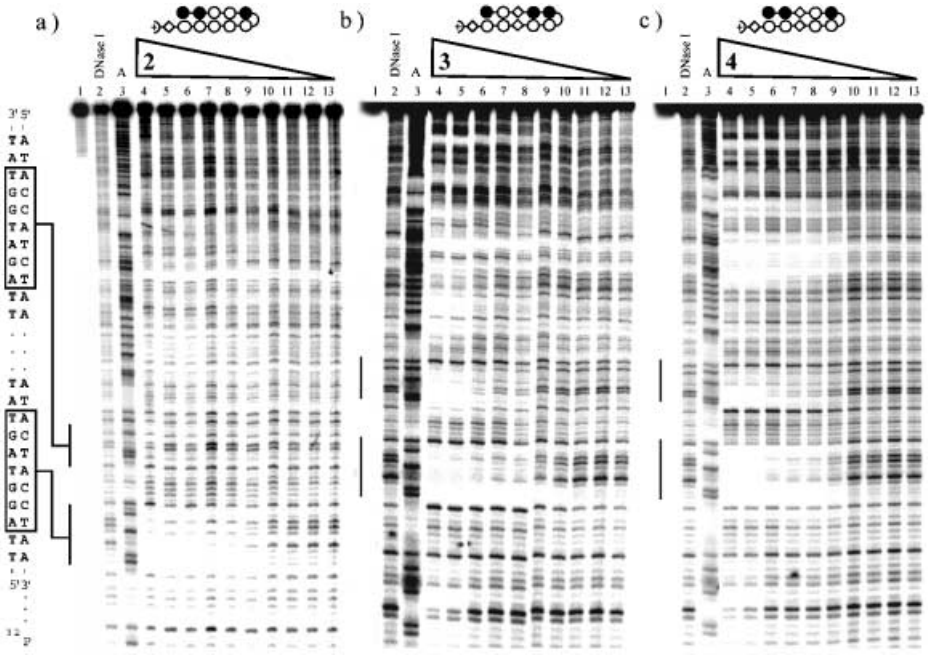

Fig. 3. *Quantitative DNase I footprint titration experiments with polyamides* **2**, **3**, *and* **4** *on the 5′-tAGGTAGTa-3′ and 5′-tAGATGGTa-3′ sites of the 3′-*^{32}*P end-labeled restriction fragment from pVR2b2. Lane 1:* intact DNA; *Lane 2:* DNase I standard; polyamide concentration *Lanes 4–13*, 50 nM, 20 nM, 1 nM, 5 nM, 2 nM, 1 nM, 0.5 nM, 0.2 nM, 0.1 nM, respectively.

Table 1. *Equilibrium Association Constants* [M^{-1}] *and Orientational Preference for Polyamides*[a])[b])

	Polyamide	5′-tAGATGGTa-3′	Orientation	5′-tAGGTAGTa-3′	Orientation
1	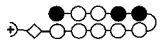	$\leq 1 \times 10^7$	N.d.	$\leq 1 \times 10^7$	N.d.
2		$\leq 1 \times 10^7$	Forward	**5.0×10^9 (1.2)**	Forward
3		**8.2×10^8 (0.8)**	Forward	**5.5×10^9 (0.3)**	Reverse
4		**2.0×10^9 (0.6)**	Reverse	4.1×10^9 (0.3)	Reverse

[a]) Values reported are the mean values obtained from three DNase I titration experiments. [b]) The assays were carried out at 22° at pH 7.0 in the presence of 10 mM *Tris*-HCl, 10 mM KCl, 10 mM $MgCl_2$, and 5 mM $CaCl_2$. N.d.: not determined (due to lack of binding). Match binding by 'pairing rules' is indicated in boldface.

binds 5′-tAGGTAGTa-3′ as a reverse 2-bp mismatch rather than a forward match (*Table 1*).

Stereochemical Control of Orientation. – Earlier studies had shown that incorporation of the (*R*)-2,4-diaminobutanoic acid residue, a chiral analog of the γ-turn, enforced the preference for 5′-3′/N–C binding of six-ring hairpins [8]. Replacement of the chiral turn (R) with the opposite configuration (*S*)-2,4-diaminobutanoic acid unit in a forward-binding six-ring context resulted in a substantial reduction in affinity. This was presumed to result from a steric clash between the floor of the minor groove and the amino group of the (*S*)-2,4-diaminobutanoic acid unit [8]. This suggests the possibility that *incorporation of the (*S*)-configuration could be employed to enforce reverse binding* similar to the effect of the (*R*)-2,4-diaminobutanoic acid unit for enforcing hairpin binding in the forward orientation.

Our series of polyamides includes 2-β-2 hairpins with preference for binding in the reverse orientation, **3** at site 5′-tAGGTAGAt-3′, and **4** at sites 5′-tAGGTAGTa-3′ (mismatch underlined) and 5′-tAGATGGTa-3′. We addressed this question of stereochemical control over orientational preference by examining both the (*R*) and (*S*) isomer of 2,4-diaminobutanoic acid incorporated into four chiral 2-β-2 hairpins corresponding to **3** and **4**. New chiral 2-β-2 hairpins **5(R)**, **5(S)**, **6(R)**, and **6(S)**, as well as their affinity-cleavage analogs **5(R)E**, **5(S)E**, **6(R)E**, and **6(S)E**, were synthesized (*Fig. 5*) and footprinted on the radiolabeled fragment of pVR2b2. The α-amino moiety within each of the chiral diaminobutanoic acid turns was acetylated to conserve overall charge. Earlier work noted that employment of the (*R*)-2,4-diaminobutanoic acid turn resulted in a 10-fold increase in polyamide binding affinity, while acetylation of the primary amino group produced ligands with binding affinities comparable to those of the parent hairpin polyamides [8]. We anticipate that our stereochemically modified hairpins will bind with affinity similar to the parents **3** and **4**, though with altered orientation preference.

Through the addition of stereochemistry, we expect to correct the orientational promiscuity of polyamides such that, in combination with the power of the pairing rules, the addition of chirality allows for the prediction that 5′-tAGATGGTa-3′ will be the forward match sequence for **5(R)**, while 5′-tAGGTAGTa-3′ now represents the reverse

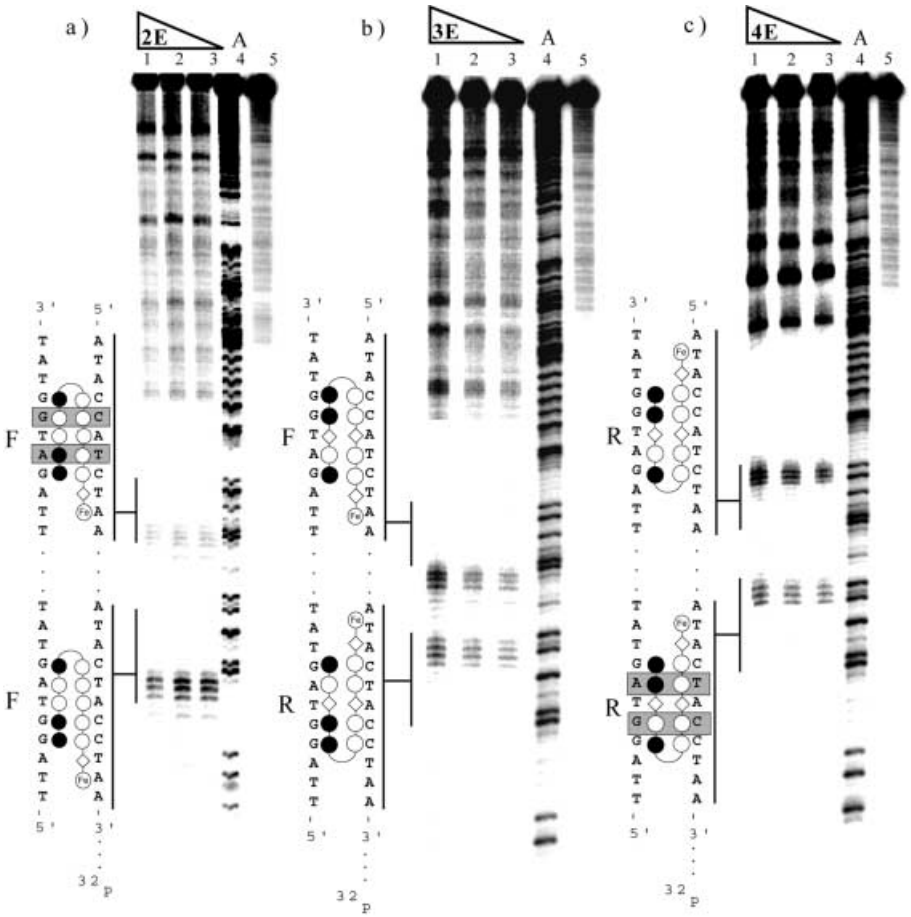

Fig. 4. *Affinity cleavage experiments on the 3′-^{32}P end-labeled restriction fragment from pVR2b2.* Sites 5′-tAGGTAGTa-3′ and 5′-tAGATGGTa-3′ are labeled with appropriately oriented ball-and-stick models of **2E**, **3E**, and **4E**. *Lanes 1–3:* polyamide-EDTA · Fe concentrations of 100 nM, 50 nM, 10 nM, respectively; *Lane 4:* A sequencing lane; *Lane 5:* intact DNA. All equilibrations performed in 25-mM *Tris* acetate buffer (pH 7.0), 10 mM NaCl, and 100 mM/base pair calf thymus DNA.

match site for hairpin **5(S)** (*Fig. 6*). The corresponding analysis for **6(R)/6(S)** allows the prediction that 5′-tAGGTAGTa-3′ represents the match DNA sequence for **6(R)**, while 5′-tAGATGGTa-3′ is the match sequence for **6(S)**. This predicted sequence specificity arises from the orientation-dependent steric interaction between the acetylated chiral turn and the floor of the DNA minor groove (*Fig. 6*).

Quantitative DNase I footprinting of **5(R)** against the restriction fragment of pV2b2 gave observed equilibrium constants of 8.6×10^9 M^{-1} for 5′-tAGATGGTa-3′ and 6.8×10^8 M^{-1} for 5′-tAGGTAGTa-3′. DNase I footprinting of **5(S)** produced the opposite trend, and we observed equilibrium association constants of 1.9×10^7 M^{-1} for 5′-tAGATGGTa-3′ and 1.2×10^9 M^{-1} for 5′-tAGGTAGTa-3′ (*Fig. 7* and *Table 2*). While

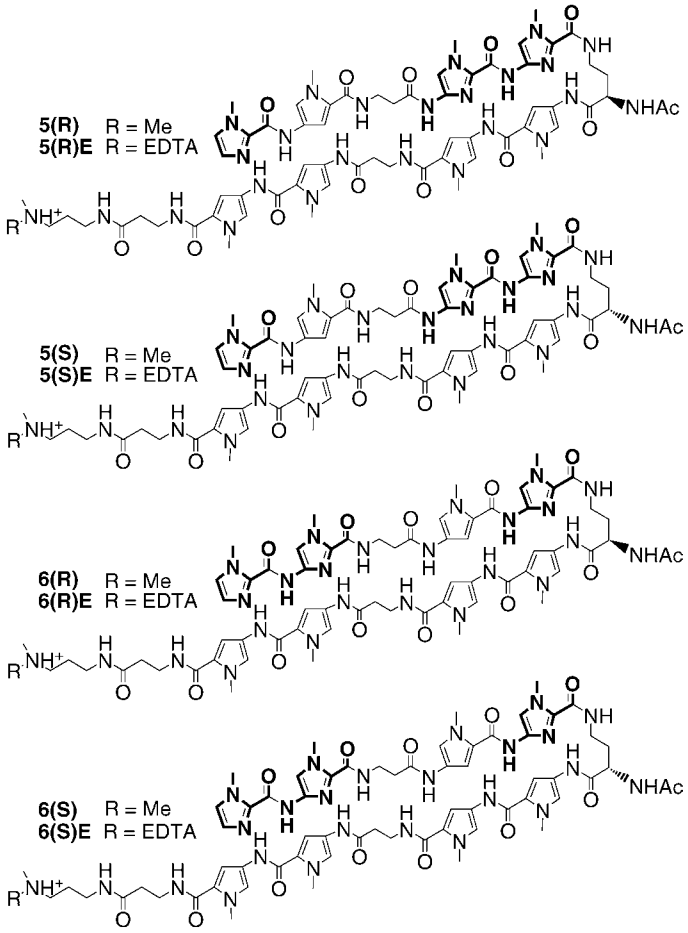

Fig. 5. *Structures of polyamides* **5R**, **5S**, **6R**, *and* **6S**

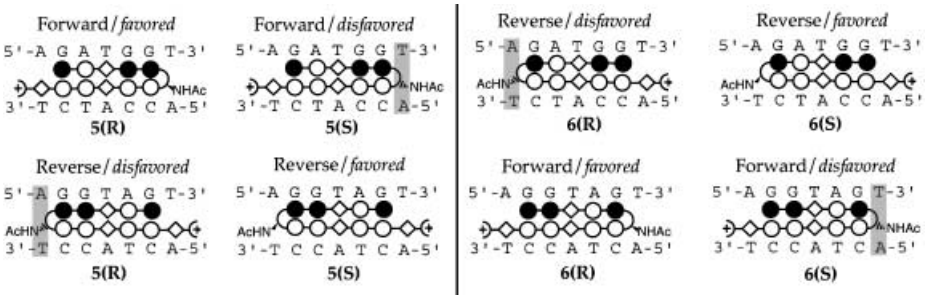

Fig. 6. Left: *Models of* **5R** *and* **5S** *in forward and reverse orientations on two sequences.* Right: *Models of* **6R** *and* **6S** *in forward and reverse orientations on two sequences.*

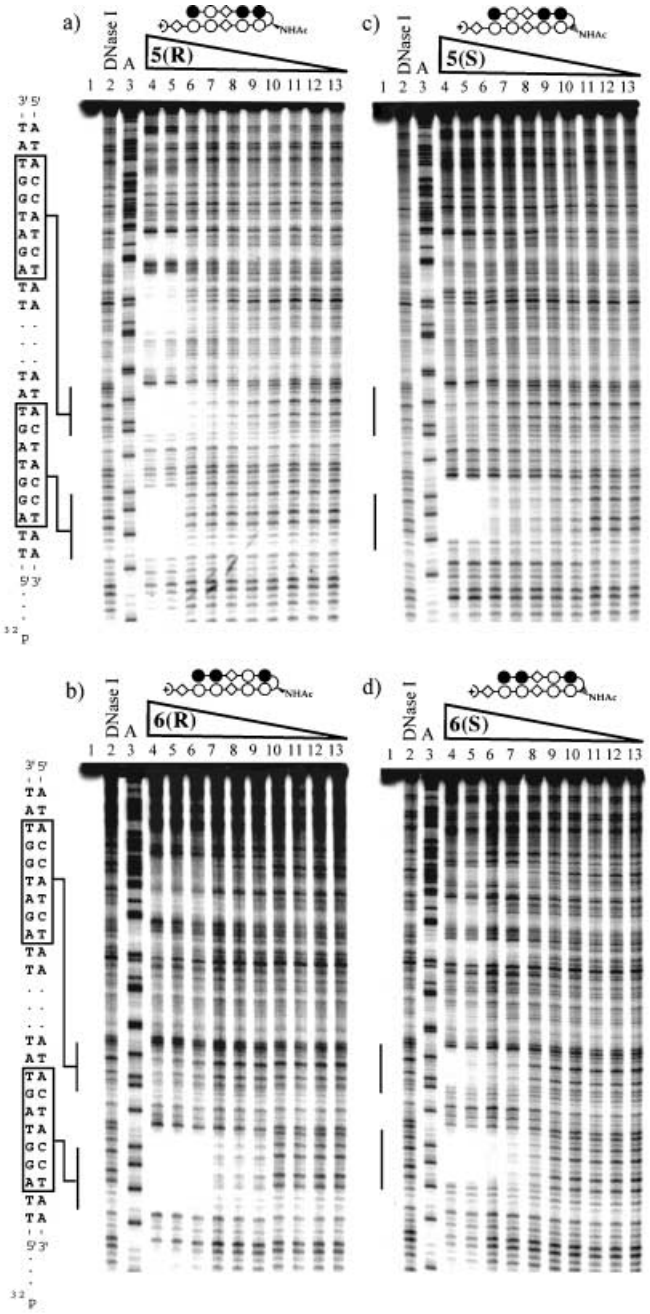

Fig. 7. *Quantitative DNase I footprint titration experiments with* **5R**, **5S**, **6R**, *and* **6S** *on the 5′-tAGGTAGTa-3′ and 5′-tAGATGGTa-3′ sites of the 5′-*^{32}*P labeled fragment from pVR2b2. Lane 1:* intact DNA; *Lane 2:* DNase I standard; *Lane 3:* A sequencing lane, polyamide concentration *Lanes 4–13:* 50 nM, 20 nM, 10 nM, 5 nM, 2 nM, 1 nM, 0.5 nM, 0.2 nM, 0.1 nM, respectively.

the parent compound, polyamide **3**, showed only modest selectivity (a sixfold preference for 5′-tAGGTAGTa-3′ over 5′-tAGATGGTa-3′), incorporation of the (*R*)-isomer reversed this trend, and hairpin **5(R)** bound site 5′-tAGATGGTa-3′ with a twelvefold preference over 5′-tAGGTAGTa-3′ while retaining excellent affinity. Polyamide **5(S)** also displayed high affinity at match sequence, 5′-tAGGTAGTa-3′, while exhibiting increased preference for 5′-tAGGTAGTa-3′ over 5′-tAGATGGTa-3′ (63-fold).

DNase I footprinting analysis of polyamide **6(R)** afforded equilibrium association constants of 2.7×10^7 M^{-1} for 5′-tAGATGGTa-3′ and 1.0×10^9 M^{-1} for 5′-tAGGTAG-Ta-3′ (*Fig. 7*, *Table 2*). In comparison to parent polyamide **4**, there is increased preference for 5′-tAGGTAGTa-3′ with respect to 5′-tAGATGGTa-3′. In accordance with the observation that hairpin polyamide **4** binds both sites in reverse orientation, it was anticipated that incorporation of the (*S*)-enantiomer of 2,4-diaminobutanoic acid would not exert a substantial effect on binding to either site. DNase I footprinting of **6(S)** indicated that this was indeed the case, and we observed equilibrium association constants of 3.0×10^8 M^{-1} and 1.3×10^9 M^{-1} for 5′-tAGATGGTa-3′ and 5′-tAGGTAG-Ta-3′, respectively.

Table 2. *Equilibrium Association Constants* [M^{-1}] *and Orientational Preference for Chiral Polyamides*[a])[b])

	Polyamide	5′-tAGATGGTa-3′	Orientation	5′-tAGGTAGTa-3′	Orientation
5(R)	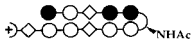	**8.6×10^9 (0.8)**	Forward	6.8×10^8 (0.3)	Forward
5(S)	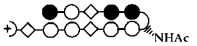	1.9×10^7 (0.8)	Forward	**1.2×10^9 (0.3)**	Reverse
6(R)	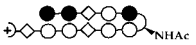	2.7×10^7 (0.6)	Forward	**1.0×10^9 (0.3)**	Forward
6(S)	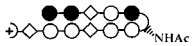	**3.0×10^8 (1.2)**	Reverse	1.3×10^9 (0.3)	Reverse

[a]) Values reported are the mean values obtained from three DNase I titration experiments. [b]) The assays were carried out at 22° at pH 7.0 in the presence of 10 mM *Tris*-HCl, 10 mM KCl, 10 mM $MgCl_2$, and 5 mM $CaCl_2$. Match binding by 'pairing rules' is indicated in boldface.

Analysis of the affinity-cleavage data for hairpins established the effect that incorporation of stereochemistry had upon orientation (*Fig. 8*). For both **5(R)** and **6(R)**, we observe binding solely in a forward orientation at both sites, indicating strong effects from the (*R*)-enantiomer in controlling polyamide orientation. This is especially interesting in light of the observation that polyamide **4** (parent to **6(R)**) binds both 5′-tAGATGGTa-3′ and 5′-tAGGTAGTa-3′ in reverse orientation. Incorporation of the (*S*)-enantiomer in polyamide **4**, *i.e.*, **6(S)**, had no effect upon orientation (*Fig. 8,d*). This result was anticipated, since, as previously mentioned, polyamide **4** bound both sites in reverse orientation. The (*S*)-enantiomer simply reinforces this preference. Hairpin **5(S)** bound 5′-tAGGTAGTa-3′ in reverse orientation and 5′-tAGATGGTa-3′ in forward orientation, thus preserving the orientational properties observed for polyamide **3**.

The Sequence Dependence of Ligand Orientation. – The design of polyamides to recognize and bind DNA sequences of increasing size has necessitated the introduction

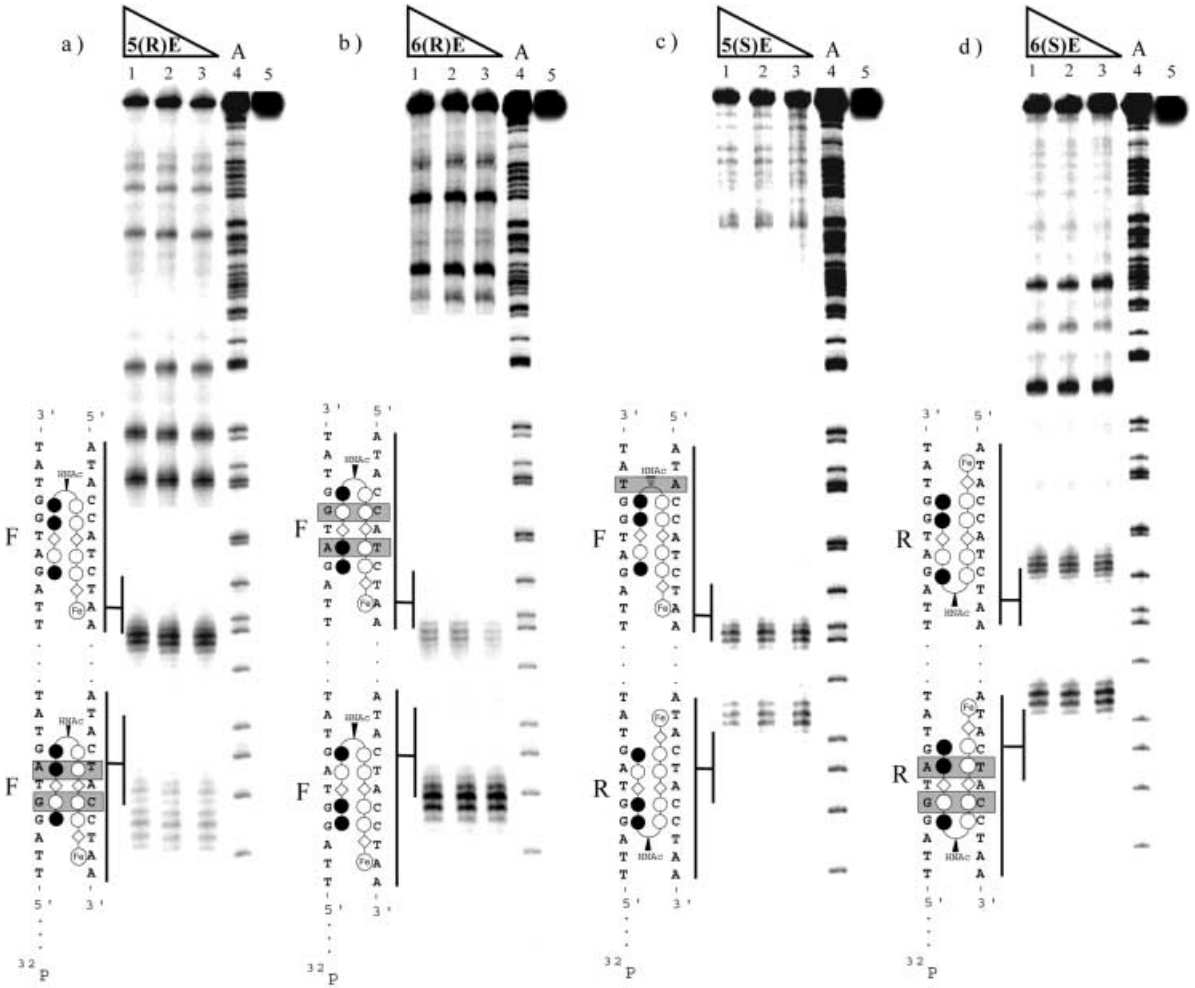

Fig. 8. *Affinity-cleavage experiments on the 5′-*^{32}*P-labeled fragment from pVR2b2 on the 5′-tAGGTAGTa-3′ and 5′-tAGATGGTa-3′ sites with appropriately oriented ball-and-stick models of* **5R**-*EDTA · Fe,* **6R**-*EDTA · Fe,* **5S**-*EDTA · Fe, and* **6S**-*EDTA · Fe. Lanes 1–3:* polyamide concentrations of 100 nM, 50 nM, 10 nM, respectively; *Lane 4:* A sequencing lane; *Lane 5:* intact DNA. All equilibrations performed in 25-mM *Tris*-acetate buffer (pH 7.0), 10 mM NaCl, and 100 μM/base pair calf thymus DNA.

of flexible units such as β-alanine that allow the polyamide to register correctly with the H-bond donor/acceptor groups displayed on the floor of the minor groove. The introduction of the β/β pair in hairpins provides ligands with increased flexibility and the ability to bind to larger DNA sequences, while maintaining affinities comparable to those of smaller six- and eight-ring DNA-binding polyamides.

Unexpectedly, the introduction of the β/β pair has limited the generality of applying the N–C/5′-3′ orientation preference displayed by polyamides containing solely aromatic amino acid pairings. This conundrum provides an impetus to determine which sequences govern forward *vs.* reverse orientation with respect to hairpin polyamide design. Introduction of the β/β pair does provide ligands with the propensity to bind in both the forward and reverse orientations, while strict retention of a Py/Py pair appears to enforce the N–C/5′-3′ orientation.

The mechanism by which the β/β pair allows or even prefers a C–N/5′-3′ orientation motif is unclear at this time and awaits more-detailed structural studies. Incorporation of β-alanine allows the polyamide to sample more conformational space in the minor groove. This would allow the optimal alignment of polyamide NH groups with the DNA bases, and, importantly, the most-favorable geometry between Im-N3 and G–NH_2 coupled with the propeller twist of G/C base pairs. In effect, the G-containing strand determines the orientational preference for a conformationally relaxed hairpin containing β/β pairs [12–15]. Due to the propeller twisting of the base pairs, the G–NH_2 group is oriented more favorably for interaction with the sp^2 orbital of Im-N3, when the polyamide is oriented N–C with respect to the 3′-5′ direction of the G-containing strand.

Implications for Polyamide Design. – The implications for polyamide design are twofold. When incorporation of a β/β pair is required to relax polyamide overcurvature to maintain binding affinity, rings (or β residues) should first be placed at the DNA sequence of interest according to the pairing rules, regardless of orientation (as in *Fig. 1*). Two hairpins connected at either end should be synthesized as candidate molecules. Either the (*R*)- or (*S*)-enantiomer of 2-(acetylamino)-4-aminobutanoic acid should then be employed to augment specificity, dependent upon the polyamide orientation desired.

Experimental Part

General. N,N′-Dicyclohexylcarbodiimide (DCC), hydroxybenzotriazole (HOBt), *O*-(1*H*-Benzotriazol-1-yl)-1,1,3,3-tetrameth yluronium hexa-fluorophosphate (HBTU), Boc-β-alanine (β), and 0.26 mmol/gram of Boc-β-alanine 4-[(carboxamido)methyl]benzyl-ester-copoly(styrene-divinylbenzene) resin (Boc-β-Pam-Resin) were purchased from *Peptides International* (*R*)-4-Boc-2-Fmoc-diaminobutanoic acid and (*S*)-4-Boc-2-Fmoc-diaminobutanoic acid were from *Bachem*. EtN(i-Pr)$_2$ (DIEA), DMF, **1**-methylpyrrolidone (NMP), DMSO/NMP, and Ac_2O, were from *Applied Biosystems*. CH_2Cl_2 and Et_3N were reagent-grade from *E. Merck*, PhSH, bis(3-aminopropyl)methylamine and 3-(dimethylamino)propylamine (Dp) were from *Aldrich*. CF_3COOH (TFA) *Biograde* was from *Halocarbon*. All reagents were used without further purification.

Quik-Sep polypropylene disposable filters were purchased from *Fisher*. A shaker for manual solid-phase synthesis was obtained from *VWR*. HPLC Analysis was performed on either a *HP 1090M* anal. HPLC or a *Beckman Gold* system with a *RAINEN* C_{18}, *Microsorb MV*, 5 μm, 300 × 4.6 mm reversed-phase column in 0.1% (*w*/*v*) TFA with MeCN as eluent and a flow rate of 1.0 ml/min, gradient elution 1.25% MeCN/min. Prep. reversed-phase HPLC was performed on a *Beckman HPLC* with a *Waters DeltaPak* 25 × 100 mm, 100 μm C_{18}

column equipped with a guard, 0.1% (*w/v*) TFA, 0.25% MeCN/min. *18MΩ* water was obtained from a *Millipore MilliQ* water purification system, and all buffers were 0.2 μm filtered. UV Spectra were measured in H_2O on a *Hewlett-Packard* model *8452A* diode-array spectrophotometer. Matrix-assisted, laser desorption/ionization time-of-flight mass spectrometry (MALDI-TOF-MS) was performed at the Protein and Peptide Micro-analytical Facility at the California Institute of Technology.

Enzymes were purchased from *Boehringer-Mannheim* and used with the supplied buffers. Deoxyadenosine and thymidine 5′-[α-^{32}P]triphosphates were obtained from *Amersham*, and deoxyadenosine 5′-[γ-^{32}P]triphosphate was purchased from *I.C.N.* Sonicated, deproteinized calf thymus DNA was acquired from *Pharmacia*. RNase-free water was obtained from *USB* and used for all footprinting reactions. All other reagents and materials were used as received. All DNA manipulations were performed according to standard protocols [16–18].

Polyamide Synthesis. Reagents and protocols for manual, solid-phase polyamide synthesis were as described in [19]. Polyamides were liberated from resin with either 3-(dimethylamino)propylamine (Dp) or bis(3-aminopropyl)methylamine at 55° for 16 h and purified by reversed-phase HPLC with *Waters DeltaPak* 25 × 100 mm, 100-μm C_{18} column equipped with a guard, and eluted with 0.1% (*w/v*) TFA, 8.0 ml/min, 0.25% MeCN/min. Affinity-cleavage analogs were synthesized as previously described. Extinction coefficients were calculated based on $\varepsilon = 8600$ M^{-1} cm^{-1}/ring at 310 nm. Compound purity and identity was verified for all compounds by anal. HPLC and MALDI/TOF MS. For **1** (monoisotopic): 1468.52 ($[M+H]^+$, $C_{69}H_{83}N_{26}O_{12}^+$; calc. 1467.64); for **2**: 1468.78 ($[M+H]^+$, $C_{69}H_{83}N_{26}O_{12}^+$; calc. 1467.64); for **3**: 1366.44 ($[M+H]^+$, $C_{63}H_{81}N_{24}O_{12}^+$; calc. 1365.62); for **4**: 1866.72 ($[M+H]^+$, $C_{63}H_{81}N_{24}O_{12}^+$; calc. 1865.62; for **5(R)**, **5(S)**, **6(R)**, **6(S)**: 1423.24 (**5(R)**), 1423.1 (**5(S)**), 1423.68 (**6(R)**), and 1423.52 (**6(S)**) ($[M+H]^+$, $C_{65}H_{84}N_{25}O_{13}^+$; calc. 1422.64).

*Construction of Plasmids pVR2b2. Bam*HI/*Hind*III restriction sites were chosen for ligation of synthetic double-stranded DNA inserts into the polylinker cloning site of pUC-19. Inserts for pVR2b2 were all provided as dry single-stranded oligonucleotides as synthesized by The Biopolymer Facility at The California Institute of Technology. The single-stranded oligonucleotides are as follows: pVR2b2, 5′-GATCCGGCCCTTAGATAG-TATGGCCCACGTTAGGTAGTATGGCCCACGTTAGATGG TATGGCCCA-3′, 5′-AGCTTGGGCCA-TACCATCTAACGTGGGCCATACTACCTAACGTGGGCCATACT ATCTAAGGGCCG-3′. Double-stranded DNA inserts were ligated in pUC-19 as per the protocol provided in the *Roche Rapid DNA Ligation Kit*. The constructed plasmids were then transformed into *Promega JM109 E. coli Subcloning Efficiency Competent Cells*. Successful ligations and transformations were chosen on the basis of blue/white screening in the presence of IPTG and X-Gal. Colonies were chosen, grown, and the plasmids were harvested with the *Promega Wizard® Plus Midiprep* purification system. Harvested plasmids were sequenced at the Nucleic Acids Sequencing Facility at The California Institute of Technology. Typical yields for purification of 75 ml of *E. coli* cells grown for 24 h at 37° in LB medium are 0.35 mg/ml.

Preparation of 3′- and 5′-End-Labeled Restriction Fragments. For 3′ label, the appropriate plasmid was linearized with *Eco*RI and *Pvu*II, then treated with the Sequenase enzyme, deoxyadenosine 5′-[α-^{32}P]triphosphate and thymidine 5′-[α-^{32}P]triphosphate for 3′-labeling. For 5′-labelling: two 20 base-pair primer oligonucleotides, 5′-AATTCGAGCTCGGTACCCGG-3′ (forward) and 5′-CTGGCACGA-CAGGTTTCCCG-3′ (reverse) were constructed to complement the pUC19 *Eco*RI and *Pvu*II sites, respectively, such that amplification by PCR would mimic the long, 3′-filled, pUC19 *Eco*RI/*Pvu*II restriction fragment. The forward primer was radiolabelled with γ-^{32}P-dATP and polynucleotide kinase, and the appropriate region was amplified with PCR. The labeled fragment (3′ or 5′) was loaded onto a 6% non-denaturing polyacrylamide gel, and the desired band was visualized by autoradiography and isolated.

Affinity Cleaving [16]. All reactions were carried out in a volume of 40 μl. A polyamide stock soln. or H_2O (for reference lanes) was added to an assay buffer where the final concentrations were: 25 mM *Tris*-acetate buffer (pH 7.0), 20 mM NaCl, 100 μM/base-pair calf thymus DNA, and 20 kcpm 3′- or 5′-radiolabeled DNA. The solns. were allowed to equilibrate for 8 h. A fresh soln. of ferrous ammonium sulfate ($Fe(NH_4)_2(SO_4)_2 \cdot 6H_2O$) (10 μM) was added to the equilibrated DNA, and the reactions were allowed to equilibrate for 15 min. Cleavage was initiated by the addition of dithiothreitol (10 mM) and allowed to proceed for 30 min. Reactions were stopped by EtOH precipitation, resuspended in 100 mM *Tris*-borate-EDTA/80% formamide loading buffer, denatured at 85° for 6 min, and the entire sample was immediately loaded onto an 8% denaturing polyacrylamide gel (5% cross-link, 7M urea) at 2000 V.

DNase I Footprinting [20]. All reactions were carried out in a volume of 400 μl. We note explicitly that no carrier DNA was used in these reactions until after DNase I cleavage. A polyamide stock soln. or H_2O (for reference lanes) was added to an assay buffer where the final concentrations were: 10 mM *Tris* · HCl buffer (pH 7.0), 10 mM KCl, 10 mM $MgCl_2$, 5 mM $CaCl_2$, and 30 kcpm 3′-radiolabeled DNA. The solns. were allowed to

equilibrate for a minimum of 12 h at 22°. Cleavage was initiated by the addition of 10 µl of a DNase I stock soln. (diluted with 1 mM DTT to give a stock concentration of 1.875 U/ml) and was allowed to proceed for 7 min at 22°. The reactions were stopped by adding 50 ml of a solu. containing 2.25M NaCl, 150 mM EDTA, 0.6 mg/ml glycogen, and 30 mM base-pair calf thymus DNA, and then EtOH-precipitated. The cleavage products were resuspended in 100 mM *Tris*-borate-EDTA/80% formamide loading buffer, denatured at 85° for 6 min, and immediately loaded onto an 8% denaturing polyacrylamide gel (5% cross-link, 7M urea) at 2000 V for 1 h. The gels were dried under vacuum at 80°, then quantitated by storage phosphor technology. Equilibrium association constants were determined as described in [16].

Quantitation by Storage Phosphor Technology Autoradiography. Photostimulable storage phosphorimaging plates (*Kodak Storage Phosphor Screen S0230* obtained from *Molecular Dynamics*) were pressed flat against gel samples and exposed in the dark at 22° for 12–20 h. A *Molecular Dynamics 400S PhosphorImager* was used to obtain all data from the storage screens. The data were analyzed by performing volume integrations of all bands using the ImageQuant v. 3.2.

We are grateful to the *National Institutes of Health* for research support (GM-27681), for a biology training grant to V. C. R. (GM19789-02), and for a postdoctoral fellowship to *C. M.* (GM19789-02). We also thank *G. M. Hathaway* for MALDI-TOF mass spectrometry.

REFERENCES

[1] J. E. Darnell, *Nature Rev.* **2002**, *2*, 740.
[2] P. B. Dervan, *Bioorg. Med. Chem.* **2001**, *9*, 2215.
[3] S. White, J. W. Szewczyk, J. M. Turner, E. E. Baird, P. B. Dervan, *Nature* **1998**, *391*, 468.
[4] A. R. Urbach, J. W. Szewczyk, S. White, J. M. Turner, E. E. Baird, P. B. Dervan, *J. Am. Chem. Soc.* **1999**, *121*, 11621.
[5] S. White, E. E. Baird, P. B. Dervan, *Chem. Biol.* **1997**, *4*, 569.
[6] S. White, E. E. Baird, P. B. Dervan, *J. Am. Chem. Soc.* **1997**, *119*, 8756.
[7] J. M. Turner, E. E. Baird, P. B. Dervan, *J. Am. Chem. Soc.* **1997**, *119*, 7636.
[8] D. M. Herman, E. E. Baird, P. B. Dervan, *J. Am Chem. Soc.* **1998**, *120*, 1382.
[9] J. J. Coull, G. He, C. Melander, V. C. Rucker, D. L. Sodora, P. B. Dervan, D. M. Margolis, *J. Virol.* **2002**, *76*, 12349.
[10] J. W. Trauger, Ph.D. Thesis, California Institute of Technology.
[11] S. E. Swalley, E. E. Baird, P. B. Dervan, *Chem.–Eur. J.* **1997**, *3*, 1600.
[12] P. B. Dervan, A. R. Urbach, in 'Essays in Contemporary Chemistry, from Molecular Structure toward Biology', Eds. G. Quinkert and M. V. Kisakürek, Verlag Helvetica Chimica Acta, Zurich, 2001, 327.
[13] S. Janssen, T. Durussel, U. K. Laemmli, *Mol. Cell*. **2000**, *6*, 999.
[14] A. R. Urbach, P. B. Dervan, *Proc. Natl. Acad. Sci. U.S.A.* **2001**, *98*, 4343.
[15] A. R. Urbach, J. J. Love, S. A. Ross, P. B. Dervan, *J. Mol. Bio.* **2002**, *320*, 55.
[16] M. Brenowitz, D. F. Senear, M. A. Shea, G. K. Ackers, *Methods Enzymol*. **1986**, *130*, 132.
[17] M. Brenowitz, D. F. Senear, M. A. Shea, G. K. Ackers, *Proc. Natl. Acad. Sci. U.S.A.* **1986**, *83*, 8462.
[18] D. F. Senear, M. Brenowitz, M. A. Shea, G. K. Ackers, *Biochemistry* **1986**, *25*, 7344.
[19] E. E. Baird, P. B. Dervan, *J. Am. Chem. Soc.* **1996**, *118*, 6141.
[20] J. W. Trauger, P. B. Dervan, *Methods Enzymol.* **2001**, *340*, 450.

Received April 14, 2003